LAMB WAVE STIFFNESS CHARACTERIZATION OF COMPOSITES UNDERGOING THERMAL-MECHANICAL AGING

Michael D. Seale* and Eric I. Madaras
* National Research Council Associate
NASA Langley Research Center
Mail Stop 231
Hampton, VA 23681-2199

INTRODUCTION

The introduction of new, advanced composite materials into aviation systems requires a thorough understanding of the long term effects of combined thermal and mechanical loading upon those materials. Analytical methods investigating the effects of intense thermal heating combined with mechanical loading have been investigated by Griffis, et al. [1] and Chen, et al. [2]. Schubbe and Mall [3] and Castelli, et al. [4] have experimentally investigated both in-phase (maximum temperature at maximum load) and out-of-phase (maximum temperature at minimum load) thermal-mechanical cycling on composites. Both authors found that the damage mechanisms and fatigue lives were dependent on test parameters as well as stress levels. Castelli, et al. [4] identified matrix dominated failure modes for out-of-phase cycling and fiber dominated damage modes for in-phase cycling.

In recent years, ultrasonic methods have been developed that can measure the mechanical stiffness of composites. To help evaluate the effect of aging, a suitably designed Lamb wave measurement system is being used to obtain bending and out-of-plane stiffness coefficients of composite laminates undergoing thermal-mechanical loading. The system works by exciting an antisymmetric Lamb wave and calculating the velocity at each frequency from the known transducer separation and the measured time-of-flight. The same peak in the waveforms received at various distances is used to measure the time difference between the signals. The velocity measurements are accurate and repeatable to within 1% resulting in reconstructed stiffness values repeatable to within 4% [5]. Given the material density and plate thickness, the bending and out-of-plane shear stiffnesses are calculated from a reconstruction of the dispersion curve.

A mechanical scanner is used to move the sensors over the surface to map the time-of-flight, velocity, or stiffnesses of the entire specimen. Access to only one side of the material is required and no immersion or couplants are required because the sensors are dry coupled to the surface of the plate. In this study, the elastic stiffnesses D_{11}, D_{22}, A_{44}, and A_{55} as well as time-of-flight measurements for composite samples that have undergone combined thermal and mechanical aging for a duration of 10,000 hours are reported.

Review of Progress in Quantitative Nondestructive Evaluation, Vol. 18
Edited by Thompson and Chimenti, Kluwer Academic/Plenum Publishers, 1999

SAMPLES

The composite materials studied were a graphite fiber reinforced amorphous thermoplastic polyimide, IM7/K3B, and a graphite fiber reinforced bismaleimide thermoset, IM7/5260. The 122-cm by 30.5-cm samples were manufactured with 16 and 32 plies and had stacking sequences of $[45/0/-45/90]_{2S}$ and $[45/0/-45/90]_{4S}$, respectively. The thermoplastic samples were all constructed with 16 plys and had a nominal thickness of 0.223 cm. The thermoset specimens contained both 16 and 32 ply architectures and had nominal thickness of 0.248 cm and 0.483 cm, respectively.

The samples were subjected to thermal-mechanical aging in either 22-kip or 50-kip capacity load frames equipped with environmental chambers which have a usable temperature range of -54 °C to +344 °C. The combined thermal-mechanical aging to which these materials are subjected must be representative of the conditions which supersonic commercial airplanes will encounter. Flights which cover takeoff, climbing to high altitudes, cruising at extreme speeds, and descending to land subject the aircraft to a wide range of temperatures and load variations.

A typical temperature-strain profile for a supersonic aircraft flight is similar to that shown in Fig. 1. The temperature profile shown is adapted from information contained in Noor and Venneri [6] and Sutton [7]. The strain profile shown is adapted from information obtained from Harpur [8]. The units of the temperature and strain have been omitted due to the fact that different areas of the aircraft are subject to differing levels of both strain and temperature. Obviously, the leading edges will be subjected to a higher temperature excursion than other portions of the plane. The skin temperature at various locations on a Mach 2.4 aircraft as well as the skin temperature as a function of Mach number and altitude can be found in Noor and Venneri [6]. The temperature profiles in Ref. 6 show skin temperatures for a Mach 2.4 flight at 60,000 feet to be in the neighborhood of 150 °C.

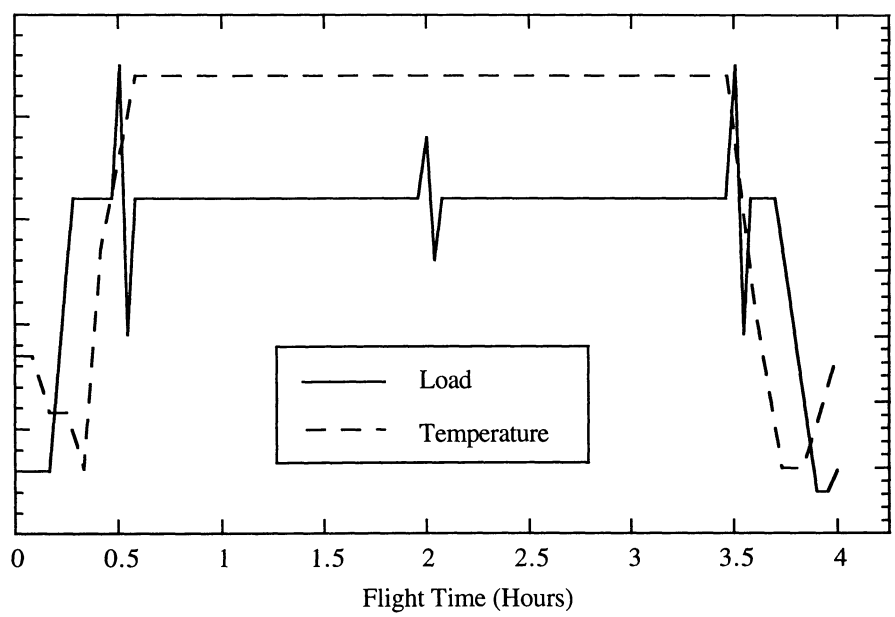

Figure 1. Typical supersonic flight profile.

In this study, the samples were subjected to either high or low strain profiles. The load levels for the low-strain samples ranged from 0 to 2,000 microstrain with a load at or above 1,040 microstrain for 180 minutes. The load levels for the high-strain samples ranged from 0 to 3,000 microstrain with a load at or above 1,560 microstrain for 180 minutes. The temperature extremes for the thermoplastic samples, IM7/K3B, were chosen to be -18 °C to +177 °C with a sustained temperature of +177 °C for 180 minutes. The temperature extremes for the thermoset samples, IM7/5260, were chosen to be -18 °C to +135 °C with a sustained temperature of +135 °C for 180 minutes. The thermoplastic samples were subjected to high strain profiles and the 16-ply and 32-ply thermoset samples were subjected to low and high strain levels, respectively.

LAMB WAVE MEASUREMENTS AND RESULTS

The Lamb wave scanning system was used to measure time-of-flight, velocity, and stiffness in the 0° and 90° directions on unaged and aged specimens. For the stiffness measurements, the sensor separation was varied from 2.75 cm to 4.75 cm in increments of 0.5 cm. A 4-cycle Gaussian-enveloped sine wave was used to generate the signal and the received signal was sampled at 25 MHz. The frequency was swept from 30 kHz to 130 kHz in 10-kHz steps and the velocity at each frequency was obtained. The thicknesses of the respective samples were given above and the density, estimated from common values for composites, was taken to be 1560 kg/m^3. From the data for the 0° measurements, the dispersion curve was reconstructed and values for the out-of-plane stiffness, A_{55}, and bending stiffness, D_{11}, were obtained. In a similar manner, the stiffnesses A_{44} and D_{22} were obtained from velocity measurements in the 90° direction.

Shown in Fig. 2 are the experimental velocity measurements in the 0° direction for an unaged thermoplastic sample and one with 10,000 hours of aging at high strain levels. Also shown are the reconstructed dispersion curves. As can be seen from the figure, the

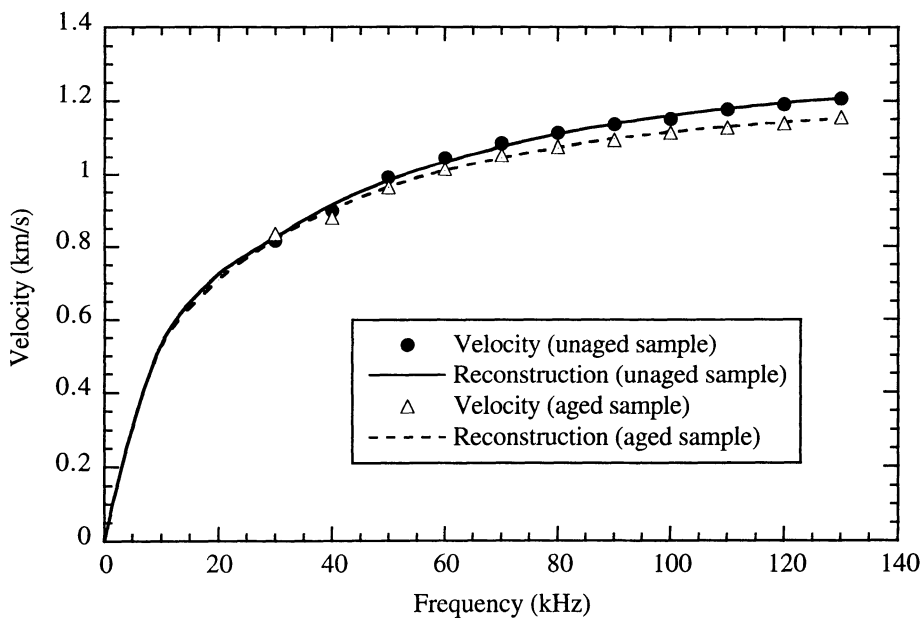

Figure 2. Experimental dispersion curves for an unaged thermoplastic sample and one aged 10,000 hours. Also shown are the reconstructed dispersion curves for each sample.

dispersion curve for the aged sample is clearly shifted from that of the unaged sample. The dispersion curves shown in Fig. 2 were reconstructed using values for the out-of-plane stiffness, A_{55}, and the bending stiffness, D_{11}, which best fit the experimental data. For the curves shown, the value of A_{55} decreased by over 12% and the value of D_{11} increased by 6% for the aged sample as compared to the unaged sample.

It is expected, and previous strain gage measurements show [9], that matrix cracking due to fatigue damage in composites leads to a decrease in elastic moduli. Since the samples were mechanically loaded as well as thermally cycled, a likely damage mechanism causing a stiffness reduction is matrix cracking. The stiffness A_{55} is controlled heavily by the matrix since the out-of-plane shear carrying capabilities of the composite are matrix dominated. Therefore, the decrease in the stiffness A_{55} is expected. However, the increase in D_{11} would not be anticipated. The reason for the increase in the value is most likely due to the insensitivity of the dispersion curve to changes in D_{11} over the measurement frequency range (30 kHz to 130 kHz). In this region, the parameter dominating the behavior of the curve will be A_{55}. Only a few data points exist at the very low frequencies (below 50 kHz) where D_{11} controls the behavior of the curve. Due to this lack of data, the constant D_{11} will be inaccurate. Therefore, the out-of-plane stiffness, A_{55}, is a more precise measurement.

Stiffness measurements were made in 45 different regions to obtain a mapping of the out-of-plane stiffness, A_{55}, for 4 thermoset samples and 2 thermoplastic samples. For each sample set, one specimen was left unaged and the other specimen was subjected to 10,000 hours of aging. The results are shown in Fig. 3. The stiffnesses have been normalized to the highest value measured in each sample set. The average normalized stiffness and standard deviation for each sample are shown in Table I. Also shown in the table are the values of D_{11} measured for each sample.

For the thermoplastic samples, the loss of stiffness with increasing aging is shown very clearly in Fig. 3. The average value of A_{55} decreased by over 10% for the aged sample

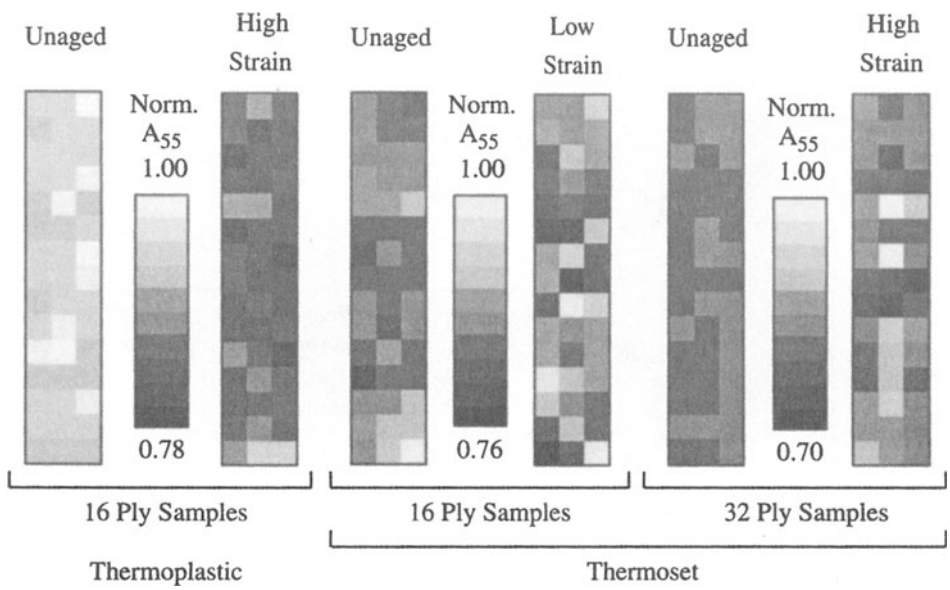

Figure 3. A_{55} stiffness mapping for composite samples which were unaged versus samples which were aged 10,000 hours at the indicated strain levels.

Table I. Normalized stiffness values in the 0° direction for aged samples.

Stiffness	16 Ply Thermoplastic		16 Ply Thermoset		32 Ply Thermoset	
Value	Unaged	High Strain	Unaged	Low Strain	Unaged	High Strain
A_{55}	0.95 ± 0.02	0.84 ± 0.02	0.86 ± 0.03	0.87 ± 0.05	0.82 ± 0.01	0.83 ± 0.05
D_{11}	0.69 ± 0.05	0.74 ± 0.10	0.75 ± 0.07	0.70 ± 0.14	0.66 ± 0.04	0.64 ± 0.12

(see Table I). The standard deviation is also observed to be only around 2% for each sample as well. In contrast, the values of D_{11} were highly variable and had deviations of up to 10% from the average. The large standard deviations associated with the average D_{11} values suggest that the measured values are not reliable. As mentioned earlier, this inaccuracy is probably due to a lack of data at low frequencies.

For the thermoset specimens, the average values of A_{55} and D_{11} did not change significantly with aging for either of the samples. What is observed from the stiffness mapping in Fig. 3, however, is an increase in the stiffness variation in the aged samples. The specimens showed localized stiffness decreases as well as localized stiffness increases. The standard deviations in the aged samples are 2 to 5 times greater than the deviations in the unaged samples (see Table I). In the thermoset samples, it is possible that the composite will continue to cure as it is heated during the aging process. This might explain the localized areas of increased stiffness which are observed. It is also possible that matrix cracking could account for the localized stiffness decreases. Coupling these two effects might explain the overall greater variability in stiffness in the aged samples. Also, consistent with the results for the thermoplastic specimens, the values of D_{11} were much more variable than the values of A_{55} for all of the thermoset samples.

Stiffness results were also obtained for values of D_{22} and A_{44} from measurements in the 90° direction. Due to the mechanical constraints of the scanner, only 18 stiffness values in the middle portion of the sample could be acquired. The results for the scans are shown in Fig. 4. As before, the stiffnesses have been normalized to the highest value obtained in each sample set. The average normalized stiffnesses A_{44} and D_{22} as well as standard deviation for each sample for the 90° measurements are shown in Table II.

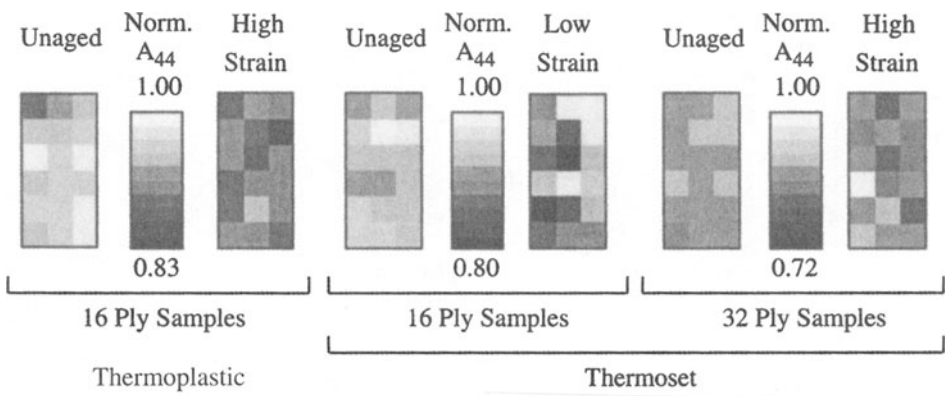

Figure 4. A_{44} stiffness mapping for composite samples which were unaged versus samples which were aged 10,000 hours at the indicated strain levels.

Table II. Normalized stiffness values in the 90° direction for aged samples.

Stiffness	16 Ply Thermoplastic		16 Ply Thermoset		32 Ply Thermoset	
Value	Unaged	High Strain	Unaged	Low Strain	Unaged	High Strain
A_{44}	0.94 ± 0.03	0.88 ± 0.02	0.94 ± 0.02	0.91 ± 0.06	0.88 ± 0.01	0.87 ± 0.04
D_{22}	0.89 ± 0.07	0.81 ± 0.08	0.81 ± 0.06	0.72 ± 0.09	0.83 ± 0.04	0.76 ± 0.08

As can be seen from the figure, the value of A_{44} decreased with increased aging for the thermoplastic sample. However, the values did not decrease as much as the values of A_{55} for this specimen. This is expected since the load was applied in the 0° direction during the aging process. Loading in this direction tends to produce cracks in the 90° plies as well as the ±45° plies. This type of damage would be indicated by a decrease in A_{55}. Since the loading occurred in the 0° direction, matrix cracking in the 0° plies probably did not occur or will not be as pronounced as in the 90° plies. Therefore, the measurement of A_{44} will only be effected by the cracks in the ±45° plies. This leads to a less significant decrease in stiffness for A_{44}, which is consistent with observation.

For the thermoset samples, the stiffness values in the 90° direction did not change significantly. However, the variability of the measured stiffnesses increased with aging. Both of these observations are consistent with the 0° measurements. Additionally, as was observed with the values of D_{11}, the values of D_{22} were highly variable and had large errors.

In addition to the stiffness measurements, time-of-flight scans in the 0° and 90° directions were conducted on the samples. A 4-cycle Gaussian-enveloped sine wave at a fixed frequency of 150 kHz was used to generate the antisymmetric Lamb wave. The scan area was 75.0 cm by 24.0 cm in the 0° direction and 25.0 cm by 24.0 cm in the 90° direction. The step size for all scans was 1.0 cm and the transducers were held fixed at a separation distance of 2.75 cm. The results for the 0° and 90° scans are shown in Figs. 5 and 6, respectively. In the figures, the values have been normalized to the lowest measured time-of-flight (fastest velocity) for each sample set. As can be seen in the figures and consistent

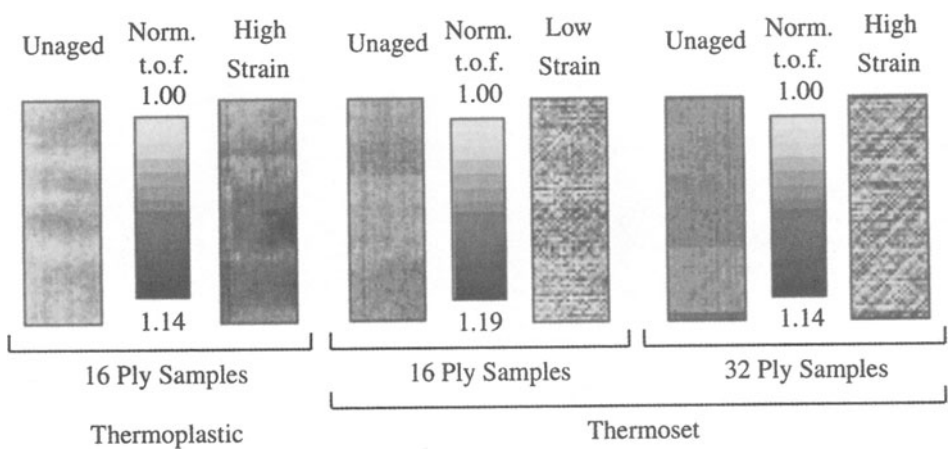

Figure 5. Time-of-flight (t.o.f.) scans in the 0° direction for composite samples which were unaged versus samples which were aged 10,000 hours at the indicated strain levels.

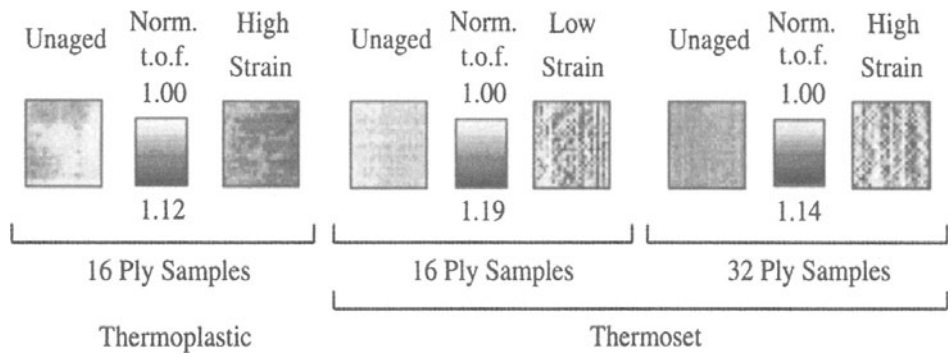

Figure 6. Time-of-flight (t.o.f.) scans in the 90° direction for composite samples which were unaged versus samples which were aged 10,000 hours at the indicated strain levels.

with the stiffness measurements, the time-of-flight is clearly shifted to longer times for the aged thermoplastic samples and becomes more variable with aging for the thermoset samples. Additionally, for the thermoset samples, the fiber structure is more observable in the aged samples. This is most likely an indication of matrix cracking along these directions.

The average time-of-flight and standard deviation for the 0° and 90° measurements are shown in Table III. As was observed in the stiffness measurements, the change in the time-of-flight in the 90° direction is less than the change in the time-of-flight in 0° direction for the thermoplastic samples. Again, this difference is most likely due to the loading in the 0° direction causing more matrix cracks to develop in the 90° plies. The thermoset samples show little to no change in average time-of-flight, but an increase in the measurement variation is observed. This trend is consistent with the variation in stiffness values measured for these samples.

DISCUSSION

Lamb wave imaging is a unique new tool for nondestructively measuring the elastic properties of a composite material. The method requires access to only one side of a specimen with no immersion or couplants. This study shows the technique to be a very effective method in providing a quantitative measure of thermal-mechanical aging in composite materials. The out-of-plane stiffness measurements in both the 0° and 90° directions correlate well with aging levels in thermoplastics. Time-of-flight scans also show a significant increase for the aged thermoplastic sample as compared to an unaged sample. This corresponds to a slower velocity, which is in agreement with the reduced stiffness measured in the aged sample. The thermoset samples did not show an overall change in stiffness. However, they did show localized changes in stiffness which may be due to damage in these areas.

Table III. Normalized time-of-flight values in the 0° and 90° directions for aged samples.

t.o.f.	16 Ply Thermoplastic		16 Ply Thermoset		32 Ply Thermoset	
Direction	Unaged	High Strain	Unaged	Low Strain	Unaged	High Strain
0°	1.03 ± 0.01	1.07 ± 0.02	1.11 ± 0.01	1.09 ± 0.03	1.08 ± 0.01	1.07 ± 0.02
90°	1.05 ± 0.01	1.07 ± 0.01	1.07 ± 0.01	1.08 ± 0.03	1.06 ± 0.01	1.05 ± 0.02

The scanning system provides a fast and accurate method of nondestructively obtaining quantitative information about materials. Such a measurement would also be sensitive to stiffness changes caused by impact damage, delaminations, fatigue, and debonds. In addition, it is reasonable to expect that this system will detect manufacturing anomalies such as inconsistent thickness, fiber misalignment, porosity, and low fiber volume fraction. This instrument provides new capabilities to inexpensively map out material properties, which is particularly useful for determining variations in material properties across a given specimen.

ACKNOWLEDGMENTS

This work was performed while the author held a National Research Council NASA-LaRC Research Associateship. The authors would also like to thank Steve Ziola, Wei Huang, and John Dorighi of Digital Wave Corporation for their technical support involving the scanning system.

REFERENCES

1. C.A. Griffis, J.A. Nemes, F.R. Stonesifer, and C.I. Chang, "Degradation in Strength of Laminated Composites Subjected to Intense Heating and Mechanical Loading," J. Composite Mater. 20, 216-235 (1986).
2. J.K. Chen, C.T. Sun, and C.I. Chang, "Failure Analysis of a Graphite/Epoxy Laminate Subjected to Combined Thermal and Mechanical Loading," J. Composite Mater. 19, 408-423 (1985).
3. J.J. Schubbe and Shankar Mall, "Damage Mechanisms in a Cross-Ply Metal Matrix Composite Under Thermal-Mechanical Cycling," in *Composites, Proceedings of the 8th International Conference on Composite Materials (ICCM8)*, Section 12-21, A92-32535 13-39, (Society for the Advancement of Material and Process Engineering, Covina, CA, 1991), pp. 20-B-1 to 20-B-9.
4. Michael G. Castelli, J. Rodney Ellis, and Paul A. Bartolotta, "Thermomechanical Testing Techniques for High-Temperature Composites: TMF Behavior of SiC(SCS-6)/Ti-15-3," NASA Technical Memorandum 103171, 1990.
5. W. Huang, S.M. Ziola, J.F. Dorighi and M.R. Gorman, "Stiffness measurement and defect detection in laminated composites by dry-coupled plate waves," in *Process Control and Sensors for Manufacturing*, edited by R.H. Bossi and D. M. Pepper, Proc. of SPIE, 3399 (1998).
6. Ahmed K. Noor and Samuel L. Venneri, senior editors, "New and Projected Aeronautical and Space Systems, Design Concepts, and Loads," in *Flight-Vehicle Materials, Structures, and Dynamics - Assessment and Future Directions*. (The American Society of Mechanical Engineers, New York, 1994), Vol. 1, pp. 15-84.
7. Sir Graham Sutton, *Mastery of the Air* (Basic Books, Inc., New York, 1965), pp. 157-166.
8. N. F. Harpur, "Concorde structural development," in *AIAA Commercial Aircraft Design and Operation Meeting*, (American Institute of Aeronautics and Astronautics, New York, 1967), No. 67-402, pp. 1-14.
9. Michael D. Seale, Barry T. Smith, and W.H. Prosser, "Lamb wave assessment of fatigue and thermal Damage in composites," J. Acoust. Soc. Am. **103** (5), Pt. 1, 2416-2424 (1998).